Available online at www.sciencedirect.com

jmr&t Journal of Materials Research and Technology

www.jmrt.com.br

Original Article

The influence of temperatures and strain rates on the mechanical behavior of dual phase steel in different conditions☆

Yu Cao, Johan Ahlström, Birger Karlsson*

Department of Materials and Manufacturing Technology, Chalmers University of Technology, SE-412 96 Gothenburg, Sweden

ARTICLE INFO

Article history:
Received 30 June 2014
Accepted 2 November 2014
Available online 3 December 2014

Keywords:
Dual phase steel
Tensile properties
Ductility
Strain rate sensitivity
Strain hardening

ABSTRACT

This study deals with the mechanical behavior of DP steel. A commercial dual phase steel (DP 800) was strained to 3.5% followed by annealing at 180 °C for 30 min to simulate the pressing of the plates and the paint-bake cycle involved in the manufacturing process of automobile body structures. The effect of temperature and strain rate on the mechanical behavior of this material was investigated by uniaxial tensile tests, covering applicable temperatures (−60 °C to 100 °C) and strain rates (1×10^{-4} to 1×10^{2} s^{-1}) experienced in automotive crash situations. Yield and ultimate tensile strength, ductility, temperature effects and strain rate sensitivity as well as strain hardening rate have been determined and discussed.

1. Introduction

Dual phase (DP) steel belongs to the family of high strength low alloy steels. It consists of a soft matrix of ferrite (F) grains with included hard martensite (M) islands. Such a microstructure provides an excellent combination of strength and ductility, making it promising for automobile applications to reduce weight of the vehicle. The mechanical properties of different DP grades have been studied by many investigators, e.g. Refs. [1–5]. This steel possesses smooth stress–strain curves with continuous yielding, low proof to tensile strength ratio, high work hardening rate and high uniform and total elongation. Static [6,7] and dynamic [2] strain aging behavior have also been reported. During low temperature bake hardening processes, both static strain aging behavior of the ferrite and tempering of the martensite have been observed. Cottrell atmospheres, carbon-clustering and precipitation can appear. It has been found by means of precision dilatometry and X-ray diffraction [7] that redistribution of carbon atoms occurs below 120 °C and precipitation of η- or ε-carbide takes place in martensite at temperatures 120–200 °C during the tempering of DP steel. Serrated stress–strain curves indicating dynamic strain aging have been observed in dual phase steel in the

☆ Paper presented in the form of an abstract as part of the proceedings of the Pan American Materials Conference, São Paulo, Brazil, July 21st to 25th 2014.

* *Corresponding author.*
E-mail: yu.cao@chalmers.se (Y. Cao).

http://dx.doi.org/10.1016/j.jmrt.2014.11.001

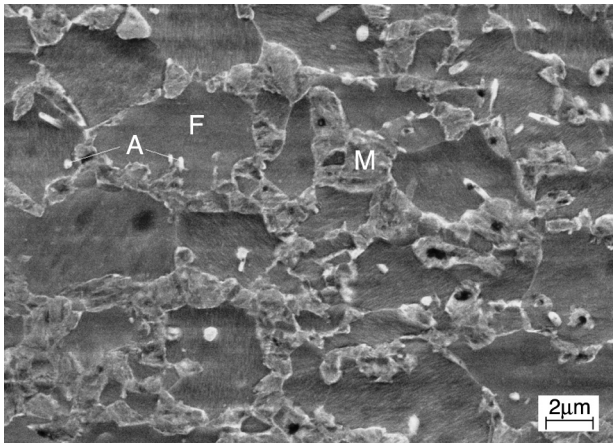

Fig. 1 – Microstructure of the studied steel. Longitudinal section perpendicular to the rolling plane. SEI image of etched specimen.

temperature range 250–450 °C [2], accompanied by increase in yield strength ($R_{p0.2}$) and ultimate tensile strength (R_m) with increasing temperature. At even higher temperature, however, $R_{p0.2}$ and R_m decrease due to softening caused by tempering of the martensite phase [8].

In the production of car bodies, pressing of the plates and the paint-bake cycle are inevitably involved. The purpose of this study was to investigate the tensile behavior of a DP steel (DP 800) exposed to these treatments, covering applicable temperatures (−60 to +100 °C) and strain rates (1×10^{-4}–$1 \times 10^{2}\ s^{-1}$) experienced in automotive crash situations. The study thus provides insight into temperature and strain rate effects on the mechanical behavior. Studied properties include yield and ultimate tensile strength, ductility, strain hardening ability as well as strain rate sensitivity.

2. Experimental

Commercial dual phase steel (DP 800) supplied by Swedish Steel AB (SSAB) in the form of rolled sheet with a thickness of 2 mm from industry regular production has been investigated. The chemical composition of the material studied is listed in Table 1. The microstructure consists of ferrite (F) grains and martensite (M) islands together with some percent of retained austenite (A), as shown in Fig. 1. The volume fraction of M is roughly 0.33. In this study, deformation to 3.5% at room temperature at a strain rate of $10^{-4}\ s^{-1}$ and subsequent heat treatment at 180 °C, 30 min in air were purposely used to simulate pressing of plates followed by the paint-bake cycle involved in the manufacturing process of automobile body structures. Prestraining to 3.5% was used since it corresponds to a strain level where approximately half of the hardening capacity up to the instability point has been exhausted and also may represent a situation where the paint-baking effect could be favorably used. Symbols AR, PS and BH are used here to represent as-received, pre-strained, as well as pre-strained and bake hardened conditions respectively.

Tensile specimens were machined with the tensile direction parallel to the original rolling direction. The strain rate was varied by more than 6 orders of magnitude, from 10^{-4} to $10^{2}\ s^{-1}$. A hydraulic Instron 8032 equipped with a temperature chamber was used for low strain rate testing up to $10^{-1}\ s^{-1}$. The testing temperature ranged from −60 °C to +100 °C with a hold time of 20 min prior to testing. High strain rate testing (up to $10^{2}\ s^{-1}$) was performed at room temperature by using an Instron VHS 8800. Detailed description of the testing procedures can be found in a previous publication [9].

The reduction in area (RA) of the materials at different strain rates and temperatures was evaluated by the equation

$$RA = \frac{A_0 - A_f}{A_0} \quad (1)$$

where A_0 is the original cross-section area and A_f the area after fracture. Digital image processing software *AxioVision* was used to measure the A_f value by outlining the fracture area under a Zeiss stereo microscope. The uniform elongation was obtained from the tensile stress–strain curve at the maximum stress. The total elongation was measured between small indentations that had been inscribed on the specimen surface prior to testing with a gauge length 40 mm.

3. Results and discussion

Fig. 2 shows engineering tensile curves at different strain rates and temperatures for the studied DP steel. Although the as-received variant (AR) exhibits continuous yielding behavior, pre-straining (PS) and superimposed bake hardening (BH) result in reappearance of a distinct yield point. Rather flat flow curves are then obtained, indicating a relatively small but approximately linear strain hardening beyond the yielding point. Increased flow stresses are observed at increased strain rates and/or decreased temperatures. This is consistent with general knowledge on the role of thermal activation upon straining. The only exception is the deformation at 100 °C. At this temperature there is a cross point of the two curves with strain rates $10^{-4}\ s^{-1}$ and $10^{-1}\ s^{-1}$ respectively, indicating a gradual change from positive to negative strain rate sensitivity with increasing strain. Clearly, an enhanced work hardening rate is obtained for low strain rates at this temperature. It is also interesting to notice the serrated stress–strain curve at the initial stage of plastic deformation, which is an indication of dynamic strain aging under this condition, as shown in Fig. 2.

The effect of the PS and PS + BH treatment on the yield and tensile strengths under different testing conditions is displayed in Fig. 3. Compared to the as-received material, PS and PS + BH treatment increase both R_m and $R_{p0.2}$ at ambient temperature, +20 °C. This is also true for the temperatures −60 °C and 100 °C. The yield strength is generally much more affected than is the ultimate tensile strength. Table 2 shows the strain hardening ratio $R_m/R_{p0.2}$, often used as a single parameter to describe strain hardening or formability in engineering terms. The data indicate that strain hardening capacity is strongly reduced by preforming and bake hardening, similarly for all temperatures and strain rates investigated.

The flow stress increase due to the PS + BH treatment is often named bake hardening arising from an aging process in the deformed material. Both Cottrell locking of dislocations

Table 1 – Chemical composition of the steel studied (wt.%).

Elem.	C	Si	Mn	P	S	Cr	Ni	Mo	Cu
Comp.	0.111	0.2	1.4	0.0091	0.0038	0.03	0.05	0.010	0.01
Elem.	V	Al	Sn	Ti	As	B	Nb	Co	N
Comp.	0.0063	0.0424	0.0029	0.0024	0.0016	0.0003	0.0136	0.015	0.0086

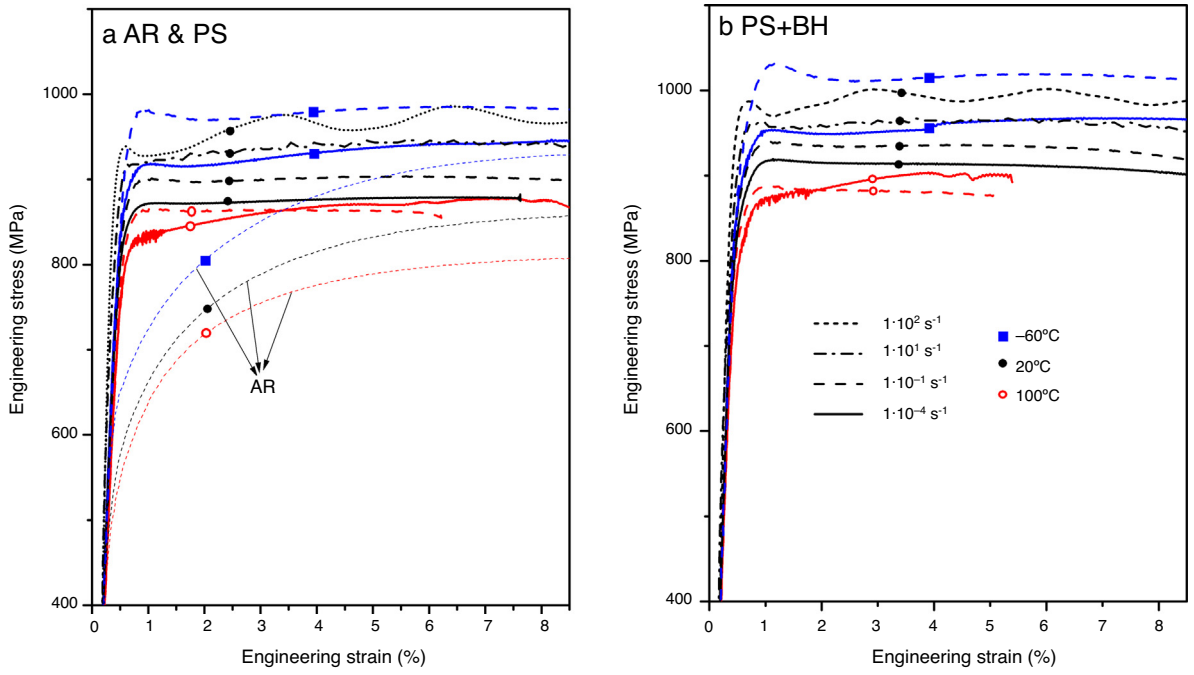

Fig. 2 – Engineering stress–strain relationships for different pre-treatments: (a) as-received (AR) and pre-strained (PS) respectively; (b) pre-strained (PS) + bake hardened (BH).

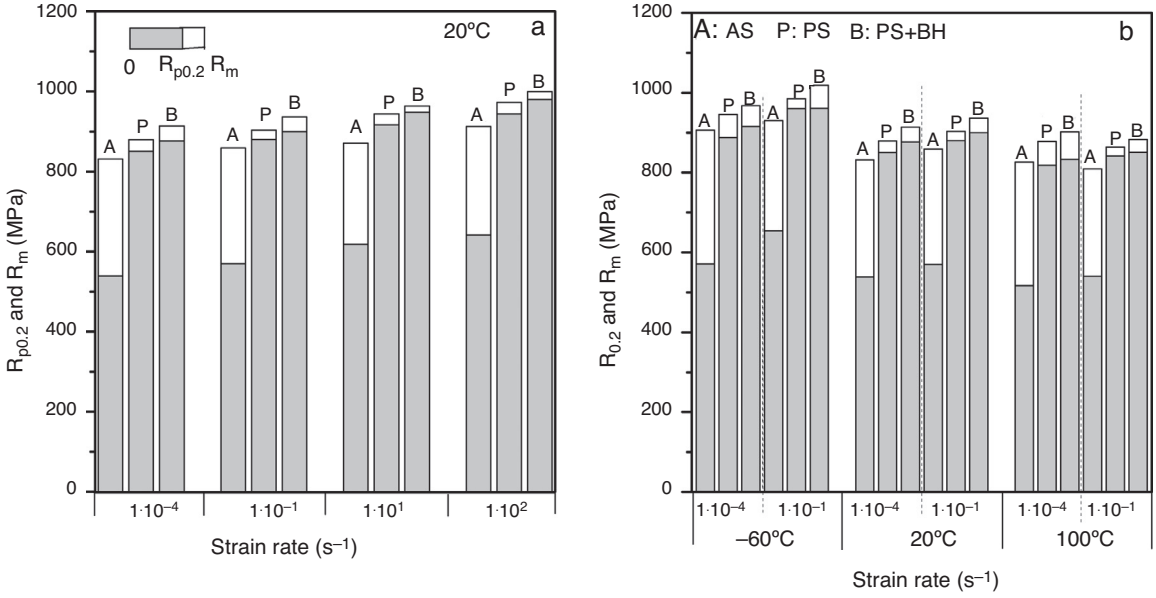

Fig. 3 – Ultimate tensile strength and yield strength of the steel studied.

Table 2 – Strain hardening ratio of the steel.

Strain rate (s^{-1})	−60 °C			20 °C			100 °C		
	AR	PS	PS + BH	AR	PS	PS + BH	AR	PS	PS + BH
10^{-4}	1.59	1.06	1.06	1.54	1.03	1.04	1.60	1.07	1.08
10^{-1}	1.42	1.03	1.06	1.51	1.03	1.04	1.50	1.03	1.04
10^{1}				1.40	1.03	1.02			
10^{2}				1.42	1.03	1.02			

and precipitation hardening can contribute to the increase of the strength in this material. Bake-hardenable steels must contain a certain minimum amount of solute carbon. During the heat-treatment at 180 °C, interstitial C diffuses to the dislocations produced during pre-straining, resulting in both a discontinuous yield point and strengthening. According to Hundy [10], dissolved C and N contents of about 0.002 wt% are sufficient to lock the dislocations. The intercritical annealing used in producing this DP steel leads to considerably higher carbon content in the ferritic phase. After completion of the first stage in which the atmosphere locking develops, carbon clusters or carbides precipitate in ferrite and martensite during the annealing [7,9,10] which further increase the resistance to the movement of free dislocations. Even though softening of martensite by tempering starts at the annealing temperature used (+180 °C), it is counteracted by the carbide formation that causes secondary hardening. The formation of fine iron carbides in martensite after bake hardening has been observed in TEM investigations [11]. In fact, carbide formation is a continuous process starting from the formation of carbon clusters as precursors followed by a compositional evolution and size growth. Therefore, the carbide formation is more sluggish than carbon diffusion. The yielding phenomenon observed after prestraining in Fig. 2a can be explained as an aging effect at ambient temperature which is less effective and caused mainly by Cottrell atmospheres. It has been reported that a clear yielding point occurs after aging in air only for 30 min in microalloyed dual phase steels [12]. The presence of fine C-rich clusters with sizes ranging from 0.7 to 2.5 nm was detected by atom probe tomography in the martensite after 4% prestraining before bake hardening [11].

The gradual change from positive to negative strain rate sensitivity with increasing strain at 100 °C can be explained as follows. The serration observed at the low strain rate $10^{-4}\,s^{-1}$ is probably related to the dynamic strain aging effects. Dislocations created during the deformation at this temperature can act as effective nucleation sites, resulting in the formation of small carbide precipitates and consequently secondary hardening. The strain hardening therefore increases. This phenomenon is time-dependent and suppressed at higher strain rate. Increased flow stress and accordingly higher ultimate tensile strength is thus obtained at low strain rate of $10^{-4}\,s^{-1}$ due to this dynamic precipitation at dislocations. An increase in work hardening rate is also expected.

The uniform elongation, total elongation and area reduction of the material are given in Figs. 4, 5, and 6 respectively. All of them are sensitive to the strain rate and temperature. Compared to the as-received materials, prestraining lowers the ductility as expected. Bake hardening (PS + BH) increases the strength at the expense of ductility.

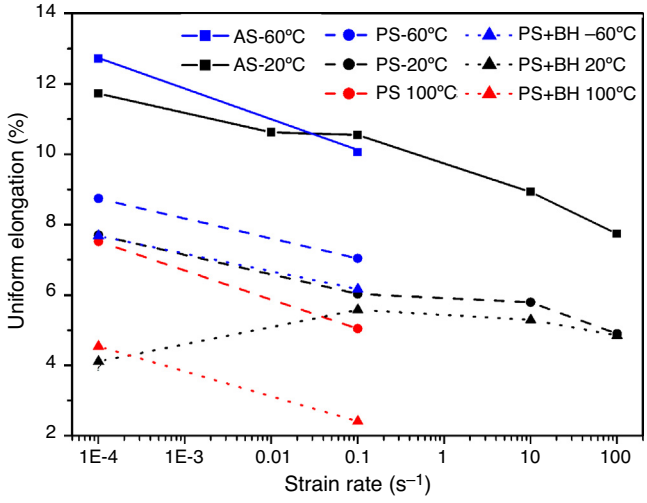

Fig. 4 – Uniform elongation as a function of strain rate and temperature.

Increasing strain rate generally lowers the uniform elongation, as shown in Fig. 4. As DP steel consists of soft ferrite grains and hard martensite islands, the latter deform mainly in an elastic way. The plastic deformation is thus conducted mostly in the ferrite matrix, giving a similar variation trend with strain rate as that of a rephosphorized steel with single ferrite phase at a given temperature [9].

Interestingly, better uniform ductility at −60 °C especially under the low strain rate $10^{-4}\,s^{-1}$ is observed. There are two possible reasons for this. In practice, the martensite reaction can never be complete, i.e., a small amount of retained austenite always remains untransformed, as shown in Fig. 1. It is metastable and has a tendency to convert to martensite (M) by plastic deformation [13], resulting in enhanced work hardening ability. The necking is thus suppressed and the uniform ductility is enhanced. The deformation temperature is a critical factor which determines the extent of the transformation. It has been observed that in the temperature range −53 to +187 °C the stability of the retained austenite is increased with testing temperature in a vanadium containing dual phase steel [14]. It should be noticed that this improvement is limited to low strain rates at −60 °C, because martensite transformation is suppressed at higher strain rate. It has been reported that even a moderate strain rate of $10^{-2}\,s^{-1}$ suppresses martensite transformation due to heating of the samples [15]. The second reason is the strain induced mechanical twinning of ferrite at low temperature, leading to an increase in strain hardening rate and consequently enhanced uniform ductility.

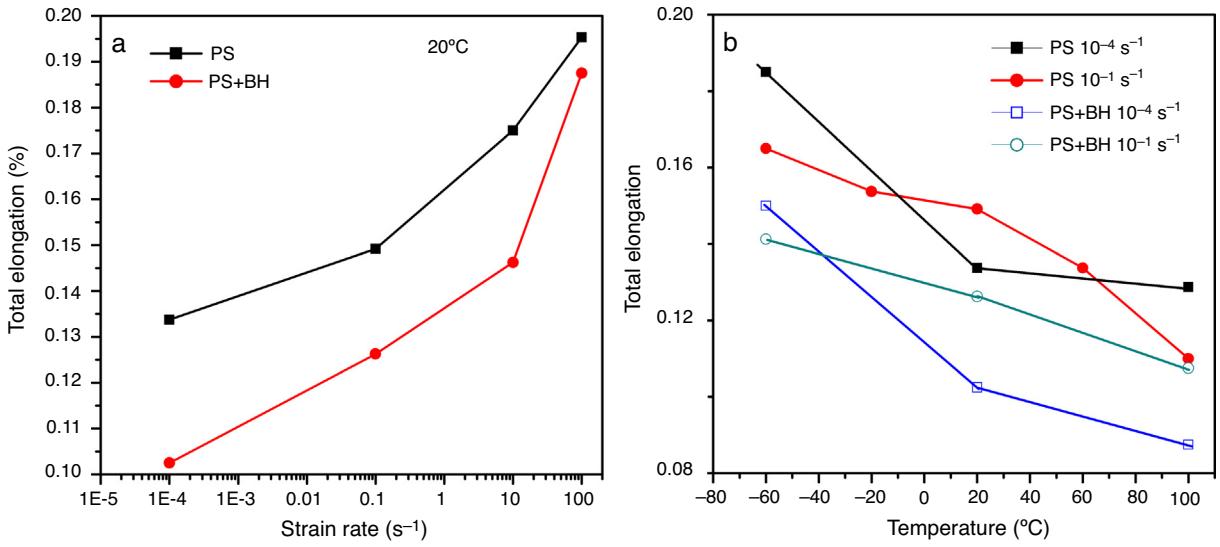

Fig. 5 – Total elongation as a function of (a) strain rate and (b) temperature. (Gauge length 40 mm.)

However, metallography observation in the present study does not reveal the existence of twinning in the ferrite grains.

Both the total elongation and area reduction increase generally with increasing strain rate at room temperature (Figs. 5a and 6a). It is opposite to the trend of uniform elongation, indicating that the local deformation at higher strain rate plays rather important role. One important reason here is that the strain rate in the neck region becomes gradually larger than the initially imposed strain rate. The increased strain hardening ability at higher stain rate, as shown later, will enhance the local deformation in the neck region and consequently total elongation and area reduction.

As to the effect of temperature, the total elongation normally increases with decreasing temperature under the conditions studied, as indicated in Fig. 5b. It is most pronounced for the lowest strain rate $10^{-4}\,s^{-1}$. This is probably again related to the strain induced transformation at lower temperatures which enhances the ductility and the development of the carbide at higher temperature which increase the strength at the expense of ductility and earlier onset of failure.

Fig. 7 shows the strain rate sensitivity β (defined by $\beta = \partial\sigma/\partial \ln \dot{\varepsilon}$) at different strain levels for the material in prestrained (PS) condition. The horizontal lines represent only the average value in the strain rate range of 10^{-4}–$10^{-1}\,s^{-1}$. β increases with decreasing temperature and increasing strain rate. At 20 °C and −60 °C, positive strain rate sensitivity is obtained. At 100 °C, however, negative strain rate sensitivity is observed when the strain is beyond a critical level, the value of which is 3.5% for the prestrained condition (PS) and 2% after additional bake hardening (PS + BH). The strain level only has minor influence on β at room temperature. At the highest and lowest temperatures (100 °C and −60 °C respectively), though, β decreases at higher strains.

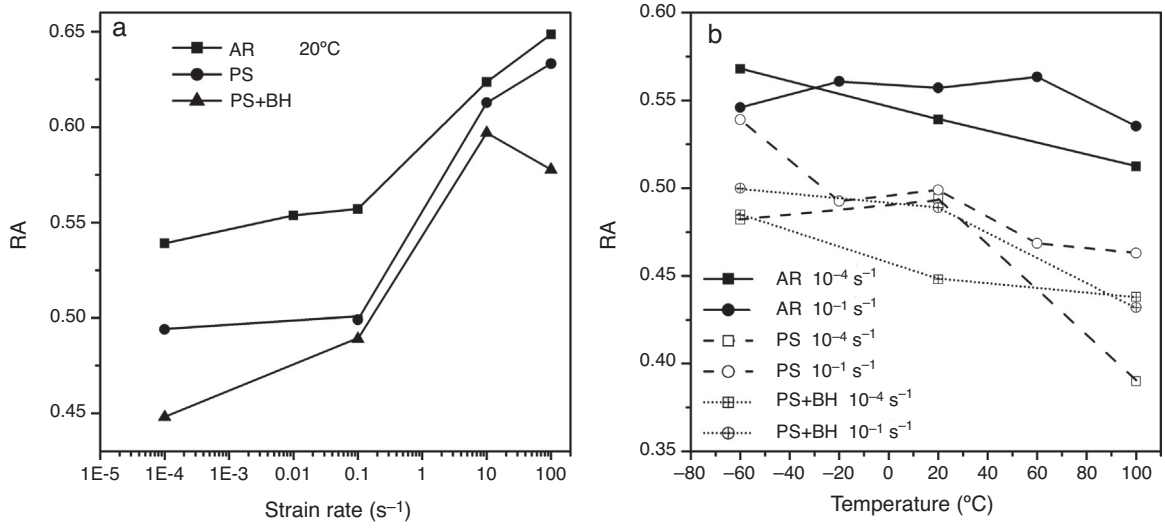

Fig. 6 – Area reduction at fracture as a function of (a) strain rate and (b) temperature.

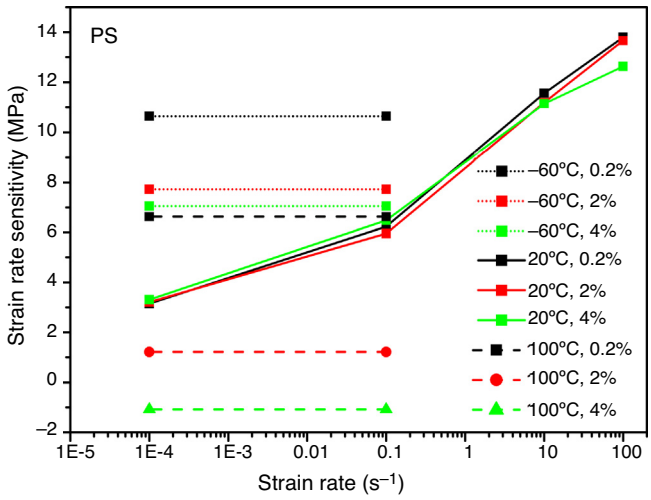

Fig. 7 – Strain rate sensitivity of the material in prestrained (PS) condition. The horizontal lines represent only the average value in the strain rate range of 10^{-4}–10^{-1} s^{-1}.

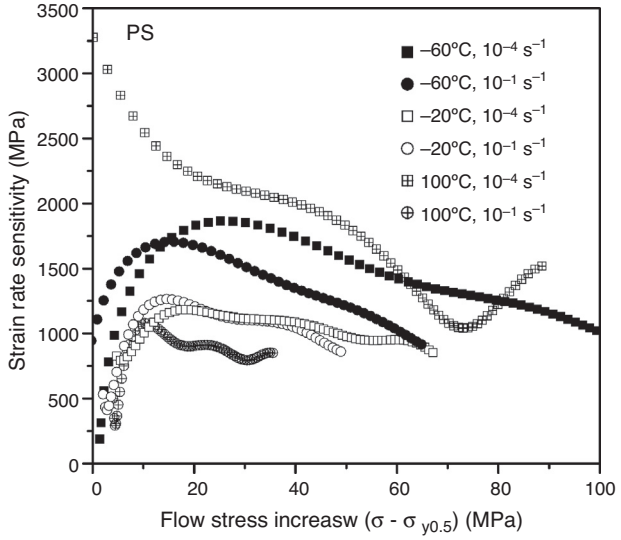

Fig. 8 – Strain hardening rate vs. flow stress increase. σ_y is the true yield stress with plastic deformation 0.5%.

The hardening characteristics of the prestrained (PS) material is given in Fig. 8, where the strain hardening rate, $\theta = d\sigma/d\varepsilon$, is plotted against the flow stress increase, $\sigma_{pl} = \sigma - \sigma_y$. Here the yield stress is defined as the stress corresponding to a plastic deformation of 0.5% in order to exclude the elastic-plastic transition. The derivative $d\sigma/d\varepsilon$ is taken by averaging the slopes of two adjacent data points on the true stress–strain curves which is fitted by high-order polynomials. The curves are cut after uniform elongation at maximum engineering stress is reached. Compared to the as received condition, as seen in Table 2, pre-deformation and further heat treatment lowers θ dramatically. With the exception of deformation at 100 °C under low strain rate of 10^{-4} s^{-1} where dynamic strain aging occurs, the hardening can be essentially considered as a two phase behavior. Normally, the strain hardening rate θ is initially low but increases to a peak value (phase I) and then decreases again (phase II). The initial phase in this case is related to the yielding event gained during the pre-treatment, giving rise to low strain hardening rates at low strains. The absence of yielding phenomenon at 100 °C under low strain rate of 10^{-4} s^{-1} results in a different initial behavior. In the second phase, θ_p systematically decreases with increasing σ_{pl}, approximately linearly, corresponding to stage three of the work hardening. Furthermore, the strain hardening rate here decreases generally with increasing strain rate at 100 and −60 °C, owing to the transformation discussed previously.

4. Conclusions

The mechanical behavior of a dual phase steel (DP 800) over a range of temperatures and strain rates has been investigated in this study. The material was characterized in the delivery state as well as after prestraining and bake-hardening. Temperatures ranging from −60 °C up to +100 °C and strain rates varying from 10^{-4} s^{-1} to 10^{2} s^{-1} were used in the experiments in order to simulate load conditions likely to occur in crash situations for automotive components. Based on the results from uniaxial tensile tests, the following principal conclusions can be drawn:

(1) Prestraining and superimposed bake-hardening lead to increased strength, decreased strain hardening, and smaller ductility at all temperatures and strain rates. In addition, prestraining leads to yield phenomena through strain aging which is further enhanced by subsequent bake-hardening.
(2) An increase in yield ($R_{p0.2}$) and ultimate tensile strengths (R_m) is generally observed when the strain rate is increased or when the temperature is decreased.
(3) For all pre-treatments, an increase in strain rate lowers the uniform elongation, while the total elongation and the reduction of area increase owing to higher strain rate sensitivity at high strain rates.
(4) The strain rate sensitivity β increases with decreasing temperature. Positive β is obtained at 20 °C and −60 °C. At 100 °C, however, there is a gradual change from positive to negative β with increasing strain. Moreover, β reduces with the accumulated plastic strain at 100 °C and −60 °C while it is less dependent on strain at room temperature.
(5) Macroscopically the hardening can be interpreted as a two phase behavior with elastically stressed inclusions of martensite in a plastic ferritic matrix.

Conflict of interest

The authors declare no conflict of interest.

Acknowledgments

Financial support was given by Swedish Agency for Innovation Systems (VINNOVA) and the Swedish Steel Producers' Association.

REFERENCES

[1] Kadkhodapour J, Ziaei Rad S. Experimental and numerical study on geometrically necessary dislocations and non-homogeneous mechanical properties of the ferrite phase in dual phase steels. Acta Mater 2011;59(11):4387–94.

[2] Ekrami A. High temperature mechanical properties of dual phase steels. Mater Lett 2005;59(16):2070–4.

[3] Jiang Z, Liu J, Lian J. A new relationship between the flow stress and the microstructural parameters for dual phase steel. Acta Metall Mater 1992;40(7):1587–97.

[4] Paruz H, Edmonds DV. The strain hardening behaviour of dual-phase steel. Mater Sci Eng 1989;A117:67–74.

[5] Winkler S, Thompson A, Salisbury C, Worswick M, Riemsdijk IV, Mayer R. Strain rate and temperature effects on the formability and damage of advanced high-strength steels. Metall Mater Trans 2008;39A(6):1350–8.

[6] Abdalla AJ, Hein LRO, Pereira MS, Hashimoto TM. Mechanical behaviour of strain aged dual phase steels. Mater Sci Technol 1999;15(10):1167–70.

[7] Waterschoot T, De AK, Vandeputte S, De Cooman BC. Static strain aging phenomena in cold-rolled dual-phase steels. Metall Mater Trans 2003;34A(3):781–91.

[8] Gündüz S, Demir B, Kaçar R. Effect of aging temperature and martensite by volume on strain aging behaviour of dual phase steel. Ironmak Steelmak 2008;35(1):63–8.

[9] Cao Y, Ahlström J, Karlsson B. Mechanical behavior of a rephosphorized steel for car body applications: effects of temperature, strain rate, and pretreatment. J Eng Mater Technol 2011;133(2):021019.

[10] Hundy BB. The strain-age hardening of mild steel. Metallurgia 1956;53:203–7.

[11] Pereloma EV, Miller MK, Timokhina IB. On the decomposition of martensite during bake hardening of thermomechanically processed transformation-induced plasticity steels. Metall Mater Trans 2008;39A(13):3210–6.

[12] Gündüz S. Static strain ageing behaviour of dual phase steels. Mater Sci Eng 2008;A486:63–71.

[13] Giordano L. Retained austenite variation in dual-phase steel after mechanical stressing and heat treatment. Mater Sci Eng 1991;A131:215–9.

[14] Sachdev AK. Effect of retained austenite on the yielding and deformation behavior of a dual phase steel. Acta Metall 1983;31(12):2037–42.

[15] Hedström P, Lindgren LE, Almer J, Lienert U, Bernier J, Terner M, et al. Load partitioning and strain-induced martensite formation during tensile loading of a metastable austenitic stainless steel. Metall Mater Trans 2009;40A(5):1039–48.